Journal of Power Sources 194 (2009) 1007–1020

Contents lists available at ScienceDirect

Journal of Power Sources

journal homepage: www.elsevier.com/locate/jpowsour

Thermodynamic analysis of diesel reforming process: Mapping of carbon formation boundary and representative independent reactions

Rajesh D. Parmar, Arunabha Kundu, Kunal Karan*

Queen's-RMC Fuel Cell Research Centre, 945 Princess Street, Kingston, Ontario K7L 5L9, Canada

ARTICLE INFO

Article history:
Received 5 May 2009
Received in revised form 8 June 2009
Accepted 9 June 2009
Available online 18 June 2009

Keywords:
Thermodynamic analysis
Diesel reforming
Gibbs minimization
Carbon free operation region
Independent reactions

ABSTRACT

This paper presents thermodynamic analysis of commercial diesel with 50 ppm sulfur content for the three common modes of reforming operations. Thermodynamic analysis is done to get boundary data for carbon formation and to get the composition of various species for all modes and entire range of operations. For steam reforming operation, steam-to-carbon (S/C) ratio equal to or greater than 2 is required for carbon-free operation in entire temperature range (400–800 °C). However, selection of S/C ratio requires the balance between maximizing the hydrogen yield and minimizing the energy input both of which increase with increasing S/C ratio. For partial oxidation operation, O_2/C ratio of 0.75 is preferable to maximize hydrogen yield but carbon formation can occur if regions of reactor experience temperatures lower than 700 °C. In case of autothermal reforming, for carbon-free operation, temperature of 750 °C, O_2/C ratio in the range of 0.125–0.25 and S/C ratio greater than 1.25 and ideally 1.75 is recommended. However, enthalpy analysis indicates that it is not possible to reach to thermoneutral point at this condition so it is better to operate O_2/C ratio 0.25 or little higher with constant heat supply. A set of three independent reactions is proposed that along with element balance equations can adequately describe the equilibrium composition of six major species—H_2, CO_2, CO, H_2O, CH_4, and C for the entire range of reforming operation.

1. Introduction

Diesel is a common fuel source for transportation application worldwide and, in the Northern communities of Canada, is the main source for electricity generation. Conversion of chemical energy of diesel into either motive power or electricity is achieved in combustion engines, which generates in addition to a known greenhouse gas – carbon dioxide – unwanted byproducts such as nitrogen oxides (NO_x) and particulate matter. A recent report in Canada has showed that health cost associated with exposure to particulate matter emissions is significant [1]. Without changing the fuel, it is possible to significantly reduce or even completely eliminate the impact of particulate emissions if hydrogen-rich stream generated from diesel reforming can be used as a fuel for low-temperature proton exchange membrane fuel cell (PEMFC) for automotive applications and for high-temperature solid oxide fuel cell (SOFC) for remote electricity generation [2–4]. It is pertinent to point out that reformed-diesel-fed-SOFCs are also being considered as auxiliary power units in transport trucks which require power to heat or to cool the cabin areas and to power electrical systems for refrigeration, lighting, computers and other electronic devices [5].

However, designing of reactor for reforming diesel into hydrogen rich stream is a challenging problem that includes finding an active, stable catalyst. Another problem is deactivation of supported-metal catalysts due to carbon/coke formation and by presence of sulfur compounds in the feed [5–8]. Carbon formation fouls the metal surfaces, blocks the catalyst support pores and voids, causes physical disintegration of catalyst support, and may also promote undesirable side reactions [4,6,7]. From operational standpoint, the objective is to identify operating conditions that avoid carbon formation and maximizes the production of hydrogen while simultaneously minimizes the formation of CO, CH_4, and other hydrocarbons. Depending on the reforming process chosen, an additional interest is to minimize the reactor energy input. Such conditions can be identified using chemical reaction equilibrium and thermo-chemical analyses.

There is limited literature on the chemical equilibrium analysis of diesel reforming processes. The work of Ahmed et al. [2] examines three diesel reforming processes – steam reforming (SR), autothermal reforming (ATR) and partial oxidation (POX) – in context of application as a reformer for solid oxide fuel cell system. Thermodynamic analysis results were presented in the form of product distribution over a wide range of temperature (300–800 °C) but for selected feed compositions, i.e. steam to carbon (S/C) and oxygen to carbon (O_2/C) ratios. For ATR operations, only three S/C ratios of 1.2,

* Corresponding author. Tel.: +1 613 533 3095; fax: +1 613 533 6637.
E-mail address: kunal.karan@chee.queensu.ca (K. Karan).

0378-7753/$ – see front matter © 2009 Elsevier B.V. All rights reserved.
doi:10.1016/j.jpowsour.2009.06.028

Table 1
Properties of diesel fuel.

Fuel	Formula	Sulfur content/wt. ppm	L.H.V./kJ mol^{-1}	F.L. Lower, Higher/vol.%	ρ/kg m^{-3}	B.P. or B.R./°C	H.V./kJ mol^{-1}	Cp/J mol^{-1} K^{-1} at 20 °C
Diesel	$C_{13.6}H_{27.1}$	50	8080	1, 6	856	120–430	47	340

L.H.V—Lower heating value; F.L. —Flammability limits; B.P. —Boiling Point; B.R. —Boiling Range; H.V. —Heat of vaporization.

1.5 and 1.8 were examined, each at two O_2/C ratios. For POX operation, only three O_2/C ratios – 0.5, 0.75 and 1.0 – and for SR operation, three S/C ratios – 1.5, 1.8 and 2.0 – were examined. Whereas the carbon formation temperature at these specified operating conditions could be derived from the product distribution data, carbon formation boundary for the entire spectrum of temperature and feed composition (defined by O_2/C and S/C ratios) was not explicitly presented.

In other studies, equilibrium compositions have been reported at conditions specific to the experimental work carried out using surrogate fuels [3,7,9–12] or particular C:H ratio [4] of diesel to compare with experimentally observed product compositions results. However, no detailed study of thermodynamic analysis of commercial diesel has been reported.

1.1. Objective

The objective of the present work is to *map* the thermodynamically defined carbon-free operational region for diesel reforming processes and examine the hydrogen yield and energy input by carrying out chemical equilibrium and enthalpy analysis. Unlike Ahmed et al.'s work wherein four feed composition for ATR, three feed composition for SR and three feed composition for POX were examined, carbon formation boundary for the entire range of feed composition covering three different reforming processes was carried out. The carbon formation boundary is determined from gas–solid chemical reaction equilibrium computations using Gibbs free energy minimization routine implemented in Matlab. In addition, the influence of pressure on carbon formation boundary is also examined. From the analysis of equilibrium composition of reaction product, it is shown that the composition of the six dominant species can be predicted by considering three independent reactions and the known elemental balance.

2. Diesel: composition and reforming reactions/products

2.1. Diesel fuel composition

Diesel fuel is a complex mixture of around 400 hydrocarbon species, some 20 organic compounds of sulfur, and additives. The distribution of the carbon number of the hydrocarbon molecules peaks in the range of 15–25 carbon atoms per molecule [13]. Diesel fuel contain mainly iso-paraffins, but also n-paraffins, mono-, di-, tri-, tetra cycloparaffins, alkylbenzenes, naphthalenes and phenanthrenes and even pyrenes [14]. Aromatic compounds may comprise 20 vol.% of the mixture. Different chemical formulae for diesel have been reported: $C_{14.342}H_{24.75}O_{0.0495}$ [15], $CH_{1.86}$ [4], $C_{13.4}H_{26.3}$ [12], $C_{13.57}H_{27.14}$ [16], $C_{16.2}H_{30.6}$ [10], $C_{13.6}H_{27.1}$ [14]. Ahmed et al. [2] performed thermodynamic analysis on commercial diesel having the same composition reported in Amphlett et al. [17], who simulated diesel composition that has similar heat of formation, Gibbs free energy and distillation curve to type D2 diesel. It has been reported that $C_{16}H_{34}$ is the predominant hydrocarbon in U.S. certified grade diesel (38.7 wt.%), however overall composition and heat of combustion of typical diesel fuel are more closely represented by dodecane [3,12]. The chemical equilibrium composition by definition is not path dependent; the final composition is simply a function of the thermodynamic state defined by temperature, pressure, and elemental composition (atomic ratios of C:H:O in the feed). In the present study, we have considered $C_{13.6}H_{27.1}$ to be representative of commercial diesel with 50 ppm sulfur content (as per European regulation 2005) [14]. The properties of commercial diesel are summarized in Table 1.

2.2. Reactions and products

The general scheme of reforming diesel with subsequent usage of the reformate in a SOFC is depicted in Fig. 1. The general idea is to operate the reformer such that reformate stream with as high hydrogen content as possible is generated while minimizing unwanted species—unreacted and unsaturated hydrocarbons. The practical reformers usually operate at temperatures greater than 600 °C to ensure that reactions proceed with sufficiently fast kinetics. Since the SOFCs are designed to operate in the 600–900 °C range, the upstream reformer may have to be operated at higher temperatures (>600 °C) in consideration of heat losses [10]. The ability to operate the reformer at thermally desirable conditions also depends on the type of the reforming process, which will influence the choice of catalyst and the product composition.

Reforming of hydrocarbons including diesel can be classified into three different types of processes—SR, POX, and ATR. Under idealized conditions, hydrocarbon is stoichiometrically converted to CO and H_2 in POX, and to CO_2 and H_2 in ATR and SR (assuming water-gas-shift [WGS]). Thus, the overall reaction can be represented as shown below:

$$\text{SR}: \quad C_nH_m + SnH_2O \rightarrow \left(\frac{m}{2} + 2n\right)H_2 + nCO_2 + (S-2)nH_2O \quad \Delta H > 0 \tag{1}$$

$$\text{POX}: \quad C_nH_m + AnO_2 \rightarrow \left(\frac{m}{2}\right)H_2 + 2AnCO \quad \Delta H < 0 \tag{2}$$

$$\text{ATR}: \quad C_nH_m + AnO_2 + SnH_2O \rightarrow nCO_2 + \left(\frac{m}{2} + 2n(1-A)\right)H_2 + (S-2(1-A))nH_2O \quad \Delta H \approx 0 \tag{3}$$

where S is steam to carbon ratio and A is oxygen to carbon ratio. From stoichiometric conversions, $S = 2$ for SR, $A = 0.5$ for POX reaction, and $S = 2(1-A)$ for ATR.

It must be recognized that the aforementioned reforming processes do not proceed with the idealized stoichiometries of Eqs.

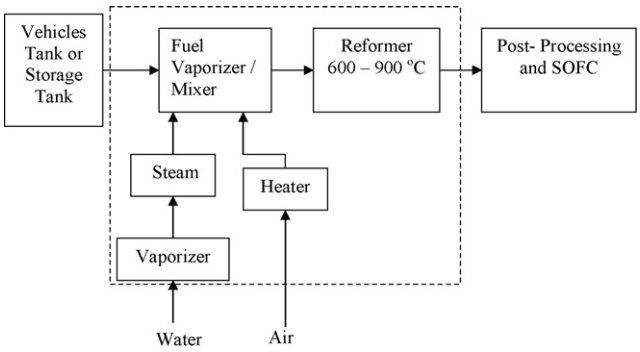

Fig. 1. Schematic diagram for reforming process and dotted line represents system boundary considered for the energy balance calculations.

(1)–(3) because of the occurrence of numerous chemical reactions – the reverse water-gas-shift reaction (RWGS), methanation, thermal cracking and gasification – shown below. As a result, the reformate streams typically contains CO, CH_4, carbon (C) and other species not included in Eqs. (1)–(3). Depending on the operating conditions and the catalyst employed, the kinetics can be sufficiently fast such that the reformate composition approaches chemical equilibrium at the given temperature and pressure. It is generally accepted that diesel reforming process involve hundreds or thousands of gas phase radical reactions as well as surface reactions. Even without the consideration of the thousands of elementary reactions, the complexity of the reforming process can be appreciated with the long list of possible key overall reactions presented below.

$$CO + H_2O \rightarrow CO_2 + H_2 \quad \Delta H^\circ = -42.2\,\text{kJ mol}^{-1} \text{ (WGS)} \tag{4}$$

$$CO + 3H_2 \rightarrow CH_4 + H_2O \quad \Delta H^\circ = -205.3\,\text{kJ mol}^{-1} \text{ (Methanation)} \tag{5}$$

$$CO_2 + 4H_2 \rightarrow CH_4 + 2H_2O \quad \Delta H^\circ = -163.1\,\text{kJ mol}^{-1} \tag{6}$$

$$2CO + 2H_2 \rightarrow CH_4 + CO_2 \quad \Delta H^\circ = -123.8\,\text{kJ mol}^{-1} \tag{7}$$

$$C_mH_n \rightarrow CH_4 + C_{m-1}H_{n-4} \tag{8}$$

$$C_mH_n + H_2 \rightarrow CH_4 + C_{m-1}H_{n-2} \tag{9}$$

$$C_mH_n \rightarrow mC + \tfrac{1}{2}nH_2 \tag{10}$$

$$CH_4 \rightarrow C + 2H_2 \quad \Delta H^\circ = 74.9\,\text{kJ mol}^{-1} \tag{11}$$

$$C_2H_2 \rightarrow 2C + H_2 \quad \Delta H^\circ = -226.9\,\text{kJ mol}^{-1} \tag{12}$$

$$C_2H_4 \rightarrow 2C + 2H_2 \quad \Delta H^\circ = -52.3\,\text{kJ mol}^{-1} \tag{13}$$

$$C_3H_6 \rightarrow 3C + 3H_2 \quad \Delta H^\circ = -20.4\,\text{kJ mol}^{-1} \tag{14}$$

$$C_4H_8 \rightarrow 4C + 4H_2 \quad \Delta H^\circ = 0.13\,\text{kJ mol}^{-1} \tag{15}$$

$$cis2 - C_4H_8 \rightarrow 4C + 4H_2 \quad \Delta H^\circ = 7.0\,\text{kJ mol}^{-1} \tag{16}$$

$$trans2 - C_4H_8 \rightarrow 4C + 4H_2 \quad \Delta H^\circ = 11.2\,\text{kJ mol}^{-1} \tag{17}$$

$$2CO \rightarrow C + CO_2 \quad \Delta H^\circ = -86.3\,\text{kJ mol}^{-1} \text{ (Boudouard)} \tag{18}$$

$$CO + H_2 \rightarrow C + H_2O \quad \Delta H^\circ = -130.4\,\text{kJ mol}^{-1} \text{ (Rev-gasification)} \tag{19}$$

$$C + O_2 \rightarrow CO_2 \quad \Delta H^\circ = -393.8\,\text{kJ mol}^{-1} \tag{20}$$

$$S + O_2 \rightarrow SO_2 \quad \Delta H^\circ = -574.3\,\text{kJ mol}^{-1} \tag{21}$$

$$SO_2 + \tfrac{1}{2}O_2 \rightarrow SO_3 \quad \Delta H^\circ = -98.9\,\text{kJ mol}^{-1} \tag{22}$$

$$SO_3 + H_2O \rightarrow H_2SO_4 \quad \Delta H^\circ = -98.2\,\text{kJ mol}^{-1} \tag{23}$$

$$H_2 + S \rightarrow H_2S \quad \Delta H^\circ = -297.3\,\text{kJ mol}^{-1} \tag{24}$$

Thermal cracking of hydrocarbon:

$$C_nH_m \rightarrow C + H_2 + CH_4 + C_2H_6 + C_3H_8 + C_4H_{10} + C_5H_{12} + C_2H_{12}\,(\text{cyclohexane}) + C_6H_6\,(\text{benzene}) + C_8H_{18}\,(\text{isooctane}) + \cdots \tag{25}$$

Hexadecane, which is major component of diesel, also reacts with O_2 [6]:

$$C_{16}H_{34} + O_2 \rightarrow C_{14}H_{10}(S) + 2CO + 12H_2 \tag{26}$$

$$C_{16}H_{34} + \tfrac{7}{2}O_2 \rightarrow \tfrac{1}{2}C_{18}H_{12}(S) + 7CO + 14H_2 \tag{27}$$

2.2.1. Carbon and coke formation

As discussed earlier, a significant problem in reforming process is the formation of carbon-rich solid phase which is often referred to as carbon and coke. The definition of carbon and coke is somewhat arbitrary and by convention related to their origin. Carbon is generally considered to be a product of CO disproportionation (Boudouard reaction; Eq. (18)) [6] while coke is produced by decomposition or condensation of hydrocarbons [6,7]. Coke forms may vary from higher molecular weight hydrocarbons such as condensed polyaromatics to carbons such as graphite, depending upon the conditions under which the coke was formed and aged [6]. In the reforming of hydrocarbons, different types of carbon or coke have been observed. Elemental carbon (whisker carbon, filamentous carbon) is formed from the decomposition of hydrocarbons (Eqs. (11)–(17)) [6,7], Boudouard reaction (Eq. (18)) and reverse gasification (Eq. (19)) [7]. Dissociation of hydrocarbons such as methane and higher hydrocarbons ($n \geq 4$) is favored at high temperatures, whereas carbon formation by Boudouard reaction and reverse gasification is favored at low temperatures. Pyrolytic carbon (Eq. (25)) is formed by thermal cracking of hydrocarbons. The formation of coke typically, not necessarily always, proceeds through the following sequence [7].

$$C_nH_m \rightarrow \text{Olefins} \rightarrow \text{Polymers} \rightarrow \text{Coke} \rightarrow \text{Amorphous carbon} \rightarrow \text{Graphitic carbon} \tag{28}$$

It should be emphasized that amorphous carbon (filamentous) is favored at low temperature (<600 °C) whereas graphitized carbon (also whisker type) is favored at high temperature (>600 °C). Compounds which approximates the structure of coke, such as anthracene ($C_{14}H_{10}$; Eq. (26)) and naphthacene ($C_{18}H_{12}$; Eq. (27)), are thermodynamically favorable even at POX conditions [7].

In a reformer system, there is a potential for coke/carbon formation in the catalytic reactor (reformer) as well as in its upstream and downstream units, for example, carbon/coke formation is possible and observed in the vaporizer unit. Furthermore, if the transfer line downstream of the reformer is not catalytically inert, carbon formation at low temperature via Boudouard reaction and reverse gasification reaction (Eqs. (18) and (19)) can occur. As such, prior to operating a reformer (lab-scale or industrial) it is useful to assess the conditions under which carbon formation is thermodynamically favored. If the reformer is operated outside this thermodynamic carbon formation region, the carbon formation may be avoided. In practice, further considerations to non-idealities, such as inadequate mixing, must be given and it must be recognized that the reformer operation may be limited by reaction kinetics.

One of the reformer process units wherein there is significant potential for carbon formation is the vaporizer or injector. It must be noted that diesel fuel is liquid at ambient conditions and would have to be either vaporized or directly injected into another reacting stream, irrespective of the type of reforming process chosen. Since diesel is a hydrocarbon mixture, it has a boiling point temperature range. The least stable components of the diesel fuel crack into free radicals at the auto-ignition temperature, which may be as low as 250 °C for some fuels. If insufficient oxygen or steam is present, the free radicals can initiate chain polymerization reactions forming carbon-rich phase or tars.

2.2.2. Sulfur compound formation

Small amount of sulfur in diesel fuel is a potential poison for many reforming catalyst, however it also minimizes coke formation [4,7]. Expected sulfur products during the reforming of sulfur containing-diesel are SO_2 and H_2S (Eqs. (21) and (24)). However SO_3 and H_2SO_4 (Eqs. (22) and (23)) may also exist at conditions encountered in the cold exhaust lines of reformer. Further, H_2S can interact with metal catalyst resulting either in surface adsorbed sul-

fur (at low H_2S concentrations) or in bulk metal sulfide (at high H_2S concentrations) [18]. The loss of catalyst activity due to presence of SO_2 and H_2S has been reported [19]. In fact, one method of catalyst selection involves the use of Ellingham diagram, which plots the Gibbs free energy of formation of various bulk sulfides as a function of temperature and H_2S/H_2 molar ratio in the system [4,7]. In the present study, we have not considered the formation of bulk metal sulfides.

2.2.3. CO and CH_4 formation

The primary goal of the hydrocarbon reforming process is to generate hydrogen, however, CO and/or CH_4 are always observed in the reformate stream and are the undesired products. Reactions involving these two species are shown in Eqs. (4)–(7). CO formation is favored at high temperature because of reverse WGS reaction (Eq. (4)), reverse methanation reaction (Eq. (5)), and methane dry reforming reaction (reverse Eq. (7)), whereas CH_4 formation is favored at low temperature (Eqs. (5)–(7)). Hence, if the reformer exhaust lines are not catalytically inert and if they are at low temperature then undesired product like CH_4 is formed. Reactions which are responsible for formation of methane from hydrocarbon fuels are Eqs. (8) and (9) [14].

2.3. Summary

In summary it can be stated that diesel is a complex mixture of myriads of hydrocarbons and its reformation to hydrogen can be attained by one of the three possible processes. From the consideration of overall reaction stoichiometries, it can be deduced that the yield of hydrogen will depend on the choice of the reforming process. Moreover, highly undesirable products such as solid carbon/coke may form in the reformer or in the upstream/downstream units depending on the operating conditions. Detailed kinetic simulation of diesel reforming process and in particular prediction of carbon-formation is complicated owing to the large number of elementary reactions that must be considered and for which the kinetic rate laws are not known. However, carbon-free operational conditions that also favor high hydrogen yield can be identified by carrying out chemical reaction equilibrium study.

3. Chemical reaction equilibrium calculations

In this work, the equilibrium composition of reacting mixture is computed by the non-stoichiometric approach, in which the equilibrium composition is found by the direct minimization of Gibbs free energy, which uses scalar parameter (Lagrange's multipliers) for a given set of species [20]. The advantages of this method are: (a) a previous selection of the possible chemical equations is not necessary, (b) no divergence appears during computation and (c) an accurate estimation of initial equilibrium composition is not necessary [21].

3.1. Governing equations

The chemical equilibrium for a system at constant temperature and pressure satisfies the following equation:

$$\mathrm{d}G_{\mathrm{total}} = -S\cdot \mathrm{d}T + V\cdot \mathrm{d}P + \sum_{\mathrm{components}} \mu_i \,\mathrm{d}n_i$$

$$= 0 \overset{\mathrm{const.}T,P}{\longrightarrow} \sum_{\mathrm{components}} \mu_i \,\mathrm{d}n_i = 0 \tag{29}$$

where, G is Gibbs free energy in Joules, S is entropy in $\mathrm{J\,K^{-1}}$, T is temperature in K, V is the volume in $\mathrm{m^3}$, P is pressure in $\mathrm{N\,m^{-2}}$, μ_i is the chemical potential of species i in $\mathrm{J\,mol^{-1}}$ and n_i is the number of moles of species i.

For equilibrium composition computation, the objective is to find the values of n_i that minimizes the value of G. From Eq. (29) total Gibbs free energy of the system is given as,

$$G_{\mathrm{total}} = \sum_{\mathrm{components}} \mu_i \bar{G}_i = \sum_{\mathrm{components}} \mu_i n_i \tag{30}$$

where $\bar{G}_i$ is the partial molar Gibbs free energy, which is equal to chemical potential.

For system comprising two phases,

$$G_{\mathrm{total}} = \sum_{\mathrm{gases}} \mu_i n_i + \sum_{\mathrm{condensed}} \mu_i n_i \tag{31}$$

$$G_{\mathrm{total}} = G_{\mathrm{gas}} + G_{\mathrm{condensed}} = \sum_{i=1}^{i=n_c} n_i(\mu_i^o + RT\ln(a_i)) + \sum_{i=n_{c+1}}^{i=n_s} \mu_i n_i \tag{32}$$

where the activity of the substance, a_i, can be given as:

$$a_i = \frac{\hat{f}_i}{f_i^o} = \frac{\hat{\phi}_i y_i P}{P^o} = \frac{n_i}{n_{\mathrm{total-gas}}}\frac{\hat{\phi}_i P}{P^o} \tag{33}$$

Considering gas phase behavior as ideal, $\phi_i \approx 1$ and standard state is taken to be 1 bar, i.e. $P^o = 1$ bar.Eq. (32) can be transformed into:

$$\frac{G_{\mathrm{total}}}{RT} = g = \sum_{i=1}^{i=n_c} n_i \left(\frac{\mu_i^o}{RT} + \ln(a_i)\right) + \sum_{i=n_{c+1}}^{i=n_s} \frac{\mu_i n_i}{RT} \tag{34}$$

$$g = \sum_{i=1}^{i=n_c} n_i \left(C_i + \ln\left(\frac{n_i}{n_{total-gas}}\right)\right) + \sum_{i=n_{c+1}}^{i=n_s} \frac{\mu_i n_i}{RT} \tag{35}$$

where $C_i = g_i^o + \ln\left(\frac{P}{P^o}\right)$, $g_i^o = \frac{\mu_i{}^o}{RT}$ and μ_i^o is the molar Gibbs free energy of species i at standard state.

The last term on the right hand side of Eq. (35) representing the solids or condensed-phase species (carbon and/or sulfur) can be either set equal to zero, if all the elements' Gibbs energy of formation is set to zero at their standard state.

Further, the elements in the system must be conserved, resulting in additional m material balance equations for m elements:

$$b_j - \sum_{i=1}^{i-n_s} a_{ji} n_i = 0 \;\; for\, j = 1, 2, \ldots\ldots, m \tag{36}$$

where a_{ji} is the number of atoms of element j in molecule i, and b_j is the total amount of element j in the mixture. Eq. (36) considers solids for element balance.

Thus, the equilibrium calculation problem is the determination of the minimum of a constrained function. In terms of Lagrange multiplier (λ), the constraint function to be minimized is:

$$f = g + \sum_{j=1}^{j=m} \lambda_j \left(b_j - \sum_{i=1}^{i-n_s} a_{ji} n_i\right) \tag{37}$$

At the minimum, the derivatives with respect to number of moles of the species are zero. Thus, the derivatives with respect to mole numbers are:

$$\frac{\partial f}{\partial n_{i,\mathrm{gases}}} = C_i + \ln\left(\frac{n_i}{n_{\mathrm{total-gas}}}\right) - \sum_{k=1}^{k=m} a_{ik}\lambda_k = 0 \quad i = 1, 2, \ldots, n_c \tag{38}$$

$$\frac{\partial f}{\partial n_{i,\mathrm{solids}}} = -\sum_{k=1}^{k=m} a_{ik}\lambda_k = 0 \quad i = n_{c+1}, \ldots, n_s \tag{39}$$

The non-linear systems of equations described by Eqs. (38) and (39) can be solved by using Newton–Raphson method. In this study, the fsolve function of Matlab™ was employed to solve the set of equations.

For each S/C and O_2/C ratio, the equilibrium composition is computed in the temperature range of 400–1000 °C at an interval of 50 °C. This gave the temperature range of 50 °C where carbon disappears. Then the calculations are repeated with increment of 0.5 °C in the observed 50 °C span. The temperature at which, the carbon content is less than 1×10^{-100} moles is reported as zero carbon for that C:H:O feed ratio.

3.2. Input data

The input data for simulation includes specification of elemental composition (dictated by the feed composition), temperature, and pressure as well as the standard state free energy of formation of all species.

The standard state free energy or chemical potential (μ_i^o) for all elemental species, e.g. C (graphite), O_2, N_2, and H_2, is set equal to zero. Accordingly, for chemical compounds $\mu_i^o = \Delta G_{f_i}^o$, i.e. standard Gibbs energy of formation of species *i*. In this work, standard Gibbs energy of formation data is obtained from JANAF data tables [22], Pamidimukkala et al. [23], and Yaws [24].

3.3. Selection of chemical species for inclusion in equilibrium calculations

For computation of equilibrium composition by free energy minimization approach, any chemical species can be included in the list of potential product (made of the constituent elements of the feed species), the thermodynamically unfavorable species simply end up with negligible mole number. However, to gain some insight into which species may be favored to exist, the free energy of formation (ΔG_f^o) of several C–H–O and sulfur species were examined as a function of temperature as shown in Figs. 2 and 3, respectively.

From Fig. 2, it can be noted that CO, CO_2 and H_2O are the most favorable oxygenated compounds. Acetaldehyde is highly unfavorable with respect to CO_2 and formaldehyde is highly unfavorable with respect to CO and CO_2. Hence these species could be possible intermediate species. C_2H_6, C_2H_4, C_2H_2, C_2H_4O, $C_{14}H_{10}$ and $C_{18}H_{12}$ are unfavorable with respect to CO, CO_2 and CH_4. Formation of $C_{14}H_{10}$, and $C_{18}H_{12}$ (as per Eqs. (26) and (27)) from hexadecane is highly favorable at all temperatures but thermodynamically it should decompose into CO, CO_2 in the presence of oxygen.

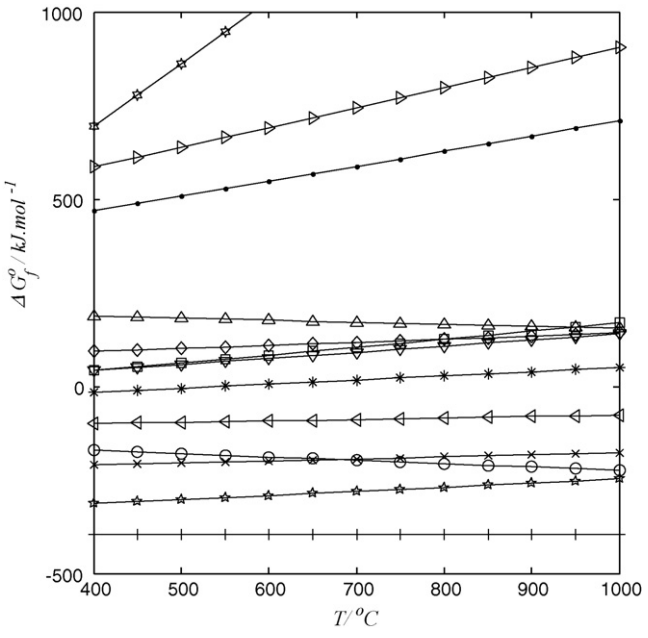

Fig. 2. Gibbs energy of formation of key carbon-containing species. ○, CO; +, CO_2; *, CH_4; ×, H_2O; □, C_2H_6; ◊, C_2H_4; △, C_2H_2; ▽, C_2H_4O; ●, $C_{14}H_{10}$; ▷, $C_{18}H_{12}$; ◁, CH_2O; ☆, CH_2O_2; ✰, $C_{16}H_{34}$.

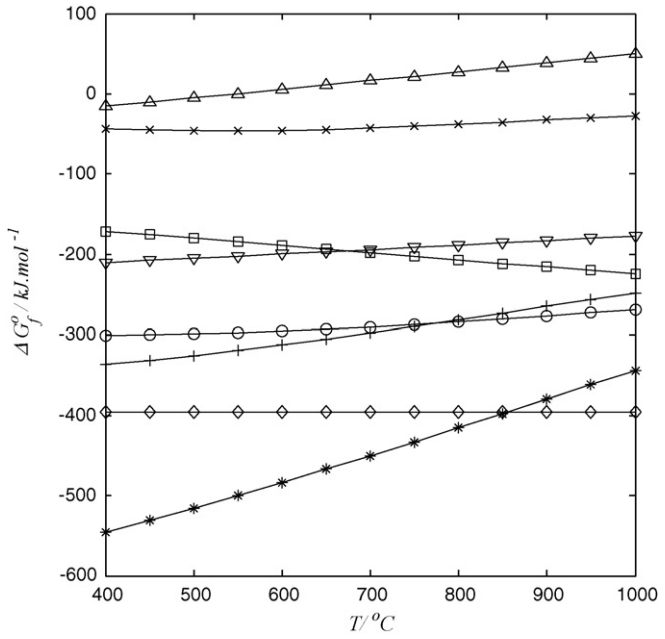

Fig. 3. Gibbs energy of formation of sulfur-containing and other key species. ○, SO_2; +, SO_3; *, H_2SO_4; ×, H_2S; □, CO; ◊, CO_2; △, CH_4; ▽, H_2O.

From Fig. 3, it can be noted that H_2SO_4 has lower Gibbs energy of formation compared to SO_2, which is lower than that for H_2S. Without considering the elemental constraints to be satisfied, it may appear that sulfur in the product will preferably be present as H_2SO_4 and SO_2 rather than H_2S. However, other oxygen-containing species must be considered in the assessing which species would be more favorable. For instance, among oxygen-containing species, thermodynamically CO_2 would be favored over both H_2SO_4 and SO_2. Thus, it would be expected that oxygen in the reaction feed would end up as CO_2 rather than SO_2 and H_2SO_4. Therefore, it may be expected that sulfur ends up as H_2S rather than H_2SO_4 or SO_2 in the equilibrium product. It must be recognized that the ultimate presence of species in the equilibrium mixture would depend, in addition to free energy of formation, on the elemental constraints imposed.

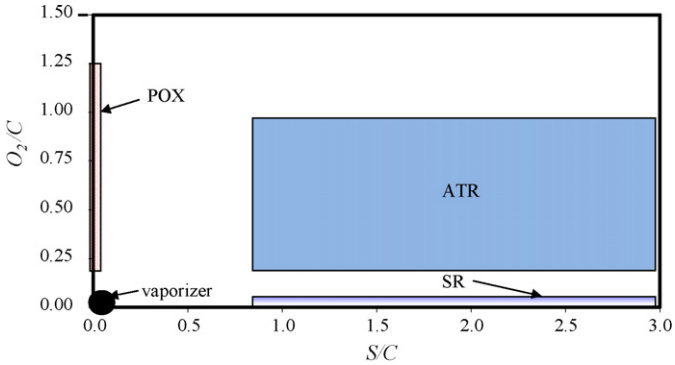

Fig. 4. Schematic representation of studied compositional operational range for various reforming processes.

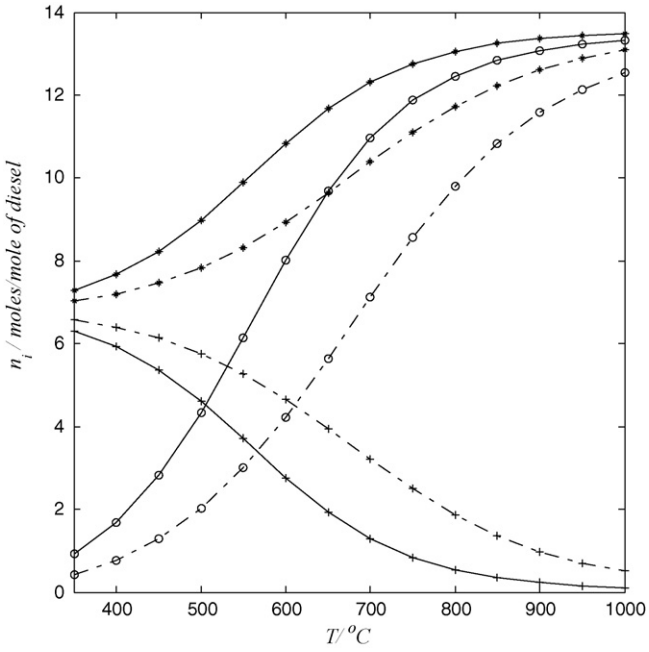

Fig. 5. Equilibrium composition in cracking of diesel. —, 1 atm; - · -, 5 atm; ◯, hydrogen; +, CH_4; *; carbon.

From the above arguments, the possible species that might be found in the final product were selected to be the following 19 species—H_2, CO, CO_2, CH_4, H_2O, O_2, H_2O, C_2H_6, C_2H_4, C_2H_2, C_2H_4O, $C_{14}H_{10}$, $C_{18}H_{12}$, SO_2, SO_3, H_2SO_4, H_2S, S (alpha (solid), beta(liquid), gamma(gas)), C (graphite). Formic acid and formaldehyde were initially added into calculations but later on removed as their equilibrium composition was very negligible (almost zero).

It is useful to point out that amorphous carbon may be favored kinetically at low temperature but thermodynamically graphite carbon is highly favorable. Reported standard Gibbs free energy change for transformation of amorphous carbon into graphite carbon varies from −11.054 to −3.220 kJ mol^{-1} [25]. Cimenti et al. [25] analyzed the equilibrium composition using thermodynamic data for amorphous carbon and graphite and it showed negligible amount of amorphous carbon as energy content of amorphous carbon is higher than that of graphite. Hence, for the current equilibrium calculations only graphite carbon was considered.

Table 2
Carbon formation boundary (temperature in °C) for different operating conditions.

	S/C						
O_2/C	0.00	0.75	1.00	1.25	1.50	1.75	2.00
At P = 1 atm							
0.00	≫1276	≫1023	974.9	711.1	64.49	583.4	238.3
0.125	≫1276	1023.4	717.3	657.0	600.4	315.4	231.9
0.25	≫1276	722.7	663.2	611.1	528.8	282.8	219.9
0.50	1276.0	624.7	570.1	443.8	292.8	229.4	187.9
0.75	678.8	514.1	371.9	273.8	217.4	178.6	149.4
1.00	584.9	300.4	230.3	178.9	150.6	125.0	104.7
1.25	396.1						
At P = 5 atm							
0.00	≫1282	≫1027.1	977.2	770.3	680.0	317.1	234.1
0.125	≫1282	1027.1	784.8	704.4	576.5	298.0	229.1
0.25	≫1282	797.0	720.9	639.3	384.5	275.8	218.3
0.50	1282.0	679.7	592.7	394.0	287.6	228.2	187.5
0.75	756.5	525.7	361.5	272.1	217.1	178.5	149.4
1.00	645.6	300.1	230.3	184.0	150.6	125.0	104.8
1.25	412.1						

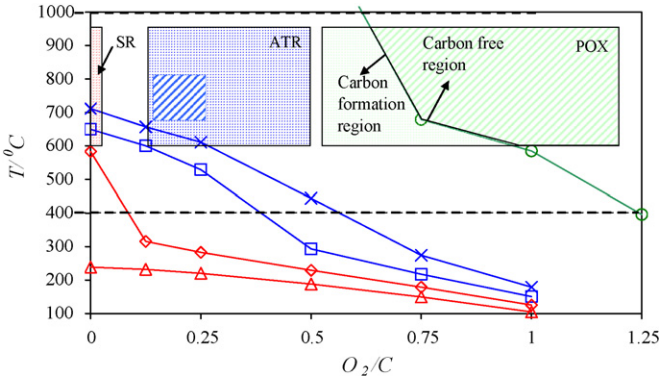

Fig. 6. Carbon formation boundary for SR, POX, and ATR at 1 atm: ◯, S/C = 0; ×, S/C = 1.25; □, S/C = 1.50; ◊, S/C = 1.75; △ S/C = 2.0. Dotted box represents thermodynamically recommended region.

4. Results and discussion

Chemical equilibrium computations were carried out to map the carbon formation boundaries in diesel reforming system and to assess the hydrogen yield in carbon-free operational region. The entire range of thermodynamic operating variables (temperature, pressure and composition) of practical interest was examined. The temperature range of interest is 400–1000 °C with the lower range relevant to the temperatures encountered in the vaporizer and the higher end temperatures expected in the exothermic partial oxidation process. For the compositional range, the steam to carbon ratio (S) and oxygen to carbon ratio (A) are parameters of interest. These ratios based on stoichiometries for SR, ATR and POX reactions of Eqs. (1)–(3) have been discussed earlier. In practical operations, values higher and lower than the ratios determined from the ideal stoichiometries are possible and, more importantly, as will be shown, necessary for carbon-free operation. The studied compositional range spanning the entire spectrum of reforming processes is indicated in Fig. 4. For fuel vaporizer

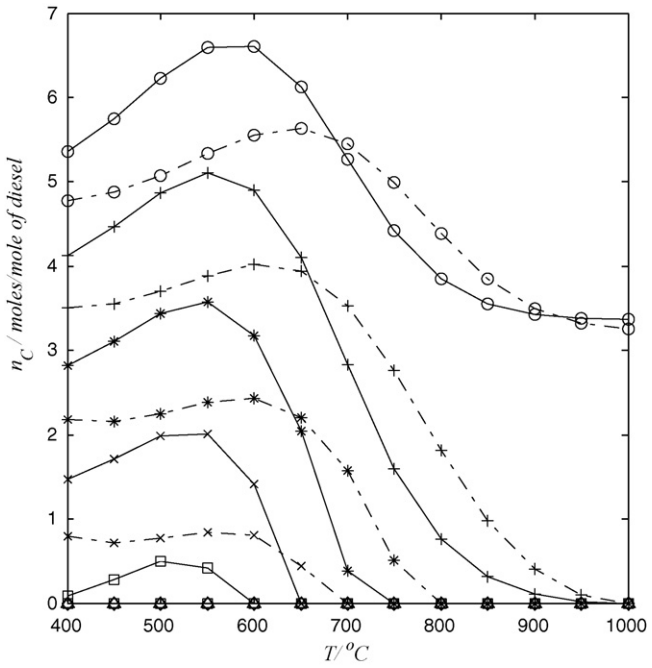

Fig. 7. Equilibrium composition of carbon in steam reforming showing the effect of system pressure. —, 1 atm; - · -, 5 atm; ◯, S/C = 0.75; +, S/C = 1.00; *, S/C = 1.25; ×, S/C = 1.50; □, S/C = 1.75.

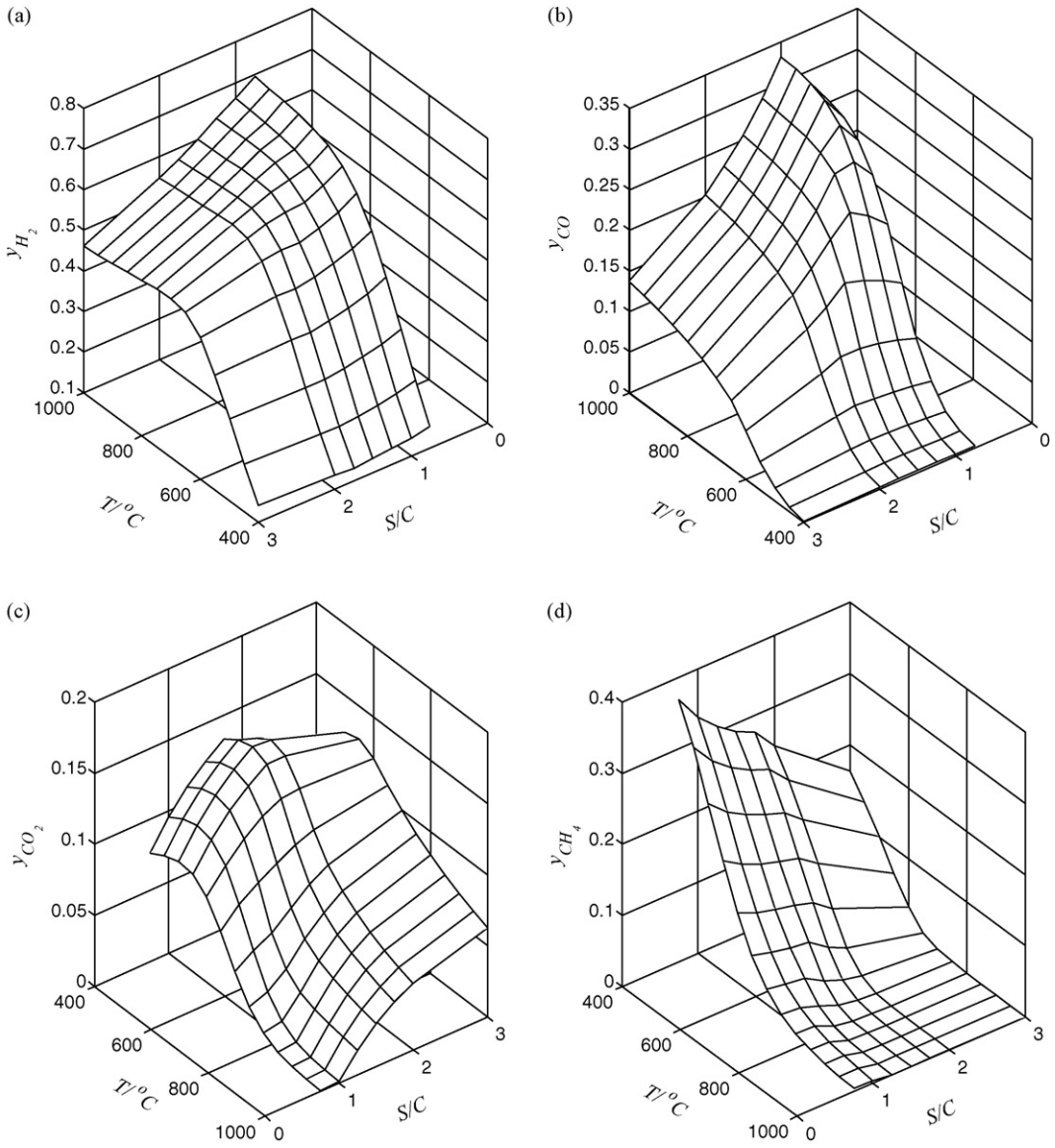

Fig. 8. Thermodynamic equilibrium gas phase product mole fraction of H_2, CO, CO_2 and CH_4 for steam reforming at 1 atm. (*Note*: for figures (a) and (b) S/C varies from 3 to 0 and for figures (c) and (d) S/C varies from 0 to 3).

where no steam and oxygen is present, the process would be depicted as a point at the origin of the plot corresponding to S/C = 0 and O_2/C = 0. It is to be noted that the vaporizer feed may be a mixture of oxidant and fuel or water and fuel, in such case the depiction of vaporizer at the origin of Fig. 4 would not be valid. Similarly, for SR process, there is no free oxygen present (O_2/C = 0) in the feed and, thereby, the operating region coincides with the *y*-axis whereas for POX process wherein no steam (S/C = 0) is present in the feed, the operating region coincides with the *x*-axis.

Finally, it is useful to remind that 19 chemical species, including condensed phases, identified in Section 3.3 were considered in all free energy minimization computations.

4.1. Carbon/coke formation boundary

Carbon formation boundary for vaporizer unit and that for various diesel reforming process is reported in this section. As discussed previously, only graphite carbon is considered in product species list and the coke, which is represented as anthracene ($C_{14}H_{10}$) and naphthacene ($C_{18}H_{12}$), is found negligible.

4.1.1. Carbon formation in vaporizer/injector

To assess the carbon formation potential in the vaporizer or injector line of the reformer, equilibrium calculations for diesel thermal cracking were carried out. All C–H species among the selected 19 species (see Section 3.3) were considered in the calculations. As expected, the dominant species were methane and hydrogen, in addition to carbon as shown in Fig. 5. It can be noted that significant amount of carbon is favored to be formed even at low temperatures. However, the kinetics of the carbon-forming reactions is likely too slow to be cause of concern. Nonetheless, if the vaporizer/injector is operated or exposed to higher temperatures—carbon formation would be favored both kinetically and thermodynamically. In case of steam reforming, it may be possible to premix the diesel with water and then vaporize the mixture. However, the immiscibility of water and hydrocarbons dictates that local composition may be significantly different than the overall composition and, thereby, result in carbon formation.

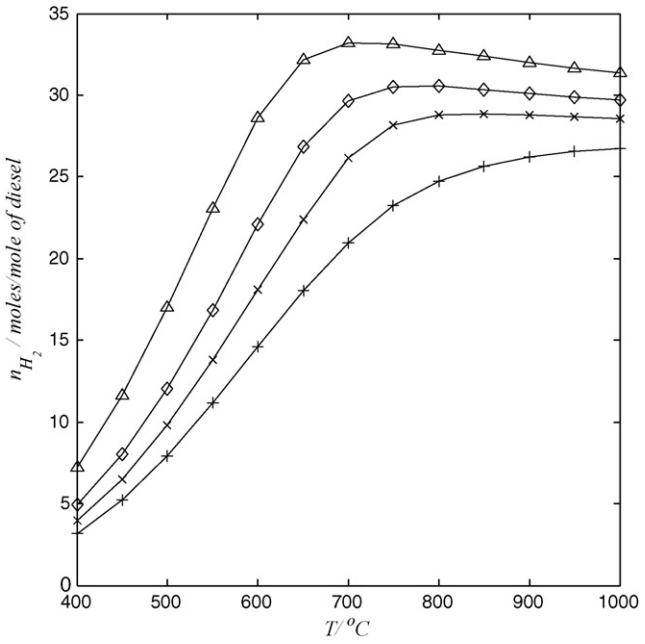

Fig. 9. Hydrogen yield for SR at 1 atm: +, S/C = 1.00; ×, S/C = 1.50; ◊, S/C = 2.00; △, S/C = 3.00.

4.1.2. Carbon formation boundary for diesel reforming processes

To map the carbon-free operational regime, based on thermodynamic consideration, carbon formation boundary over the entire range of operating conditions spanning the three different diesel reforming processes was computed. The results are presented in Table 2 wherein the carbon formation boundary temperatures at two different pressures is provided and in Fig. 6 where carbon formation boundary for various steam to carbon (S/C) ratios is shown. In Fig. 6, for a given S/C ratio, the region on the right-side or above the line represents the carbon-free conditions. Fig. 6 also shows (as boxes) the potential range of operating conditions for the three different diesel reforming processes—SR, POX and ATR. The part of the box filled with hatched line then denotes the carbon-free operational conditions for typical reforming operation.

For steam reforming (O_2/C = 0), it can be concluded from Fig. 6 that if S/C ratio is greater than 1.75, the operation is thermodynamically predicted to be carbon free for the expected operational temperature (600–800 °C). A much lower S/C ratio (∼1.25) can be tolerated if the operational temperature is 800 °C. On the other hand, for partial oxidation (S/C ratio = 0), carbon-free operations is possible for the complete operational temperature range (600–1000 °C) as long as the O_2/C ratio is higher than 1.1. However, higher O_2/C ratio can have adverse affect on hydrogen yield as will be discussed in Section 4.2.2. Similarly, the choice of S/C ratio for SR operations will also be influenced by energy input requirements and hydrogen yields.

For ATR operations, considering the possible operational region to be O_2/C ratio of 0.25–0.5 and temperature range of 600–1000 °C, it can be noted from Fig. 6 that carbon-free operations are predicted if S/C ratio of 1.5 or higher is maintained. Again, a lower S/C ratio is tolerable if the operating temperatures are on the higher end. For example, if the ATR operates at 900 °C, a S/C ratio of 1.0 is indicated to allow carbon-free operation. Apart from considerations of carbon-free operations, the choices of O_2/C and S/C ratios would further depend on the desire to maximize hydrogen yield and to operate near the thermoneutral point. The latter points are discussed in Sections 4.2 and 4.3.

4.1.3. Influence of pressure on the carbon formation boundary in SR process

The reforming operations may occur at pressures higher than atmospheric. It was of interest to get insight into the influence of pressure on the carbon-forming boundaries. Recognizing multiple variables (S/C and O_2/C ratios, temperature) and their wide range spanning different diesel reforming processes, computations were carried out for a single diesel reforming process – steam reforming – at various S/C ratio and two pressures—1 and 5 atm. It is recognized that 5 atm may be significantly higher pressure than those being considered for diesel reforming but it was chosen so as to easily discern the influence of pressure on carbon formation behavior. The amount of carbon formed as a function of temperature is presented in Fig. 7. The carbon formation boundaries can be noted as the intercept of plot with the *x*-axis. A number of interesting observations can be made from the Fig. 7. First, it can be deduced that the carbon-formation boundary temperature increases with increase in pressure. A shift of nearly 50 °C is observed for S/C ratios lower than 1.75. Second, it can be observed that the effect of pressure on the amount of carbon formed at lower temperature is opposite to that at higher temperatures for a fixed S/C ratio. It is useful to mention that similar thermodynamic trends are observed for carbon formation boundary at various temperatures and pressures for POX and ATR processes.

In principle, by the very nature of free energy minimization approach these effects cannot be explained simply in terms of reactions because a large number and combination of independent reactions can describe the observed equilibrium. However, if we consider the carbon formation/consumption to occur by the known reaction pathways described by the dissociation of hydrocarbons (Eq. (10)), Boudouard reaction (Eq. (19)) and gasification reaction (Eq. (20)), then the observed behavior can be explained as follows. As the temperature is increased, more carbon is formed because of dissociation of hydrocarbons (Eq. (10)), however at high temperature, reverse Boudouard reaction (Eq. (19)) and gasification reaction (Eq. (20)) consume carbon. Thus, it can be thought that these equilibrium reactions determine the moles of carbon over the temperature range.

The different influences of pressure at low and high temperatures can be explained by considering the simultaneous occurrence of the reactions (Eqs. (11)–(19)). It was argued above that the Boudouard and Reverse gasification reactions are responsible for formation of carbon at low temperature. At high pressure, these reactions should yield higher amount of carbon. However it is observed that, at low temperature, there is a lower amount of carbon at high pressure, which is in contradiction with our previous argument. So only the reactions which could consume the carbon are reverse dissociation reactions (Eqs. (11)–(17)). Among Eqs. (11)–(17), it can be shown that the thermodynamic behavior of carbon formation at various temperatures and pressures could be represented by one independent Eq. (11).

4.2. Hydrogen yield and product composition of diesel reforming

As stated above, identifying the conditions for carbon-free operation is only one of the metrics for determining the operational regime for reforming processes. Hydrogen yield, defined as moles of hydrogen produced per mole of diesel in the feed is another metric. Furthermore, it is useful to gain understanding of the distribution of other chemical species in the reformate stream. In the following sub-sections, the equilibrium hydrogen yield and product compositions for each of the three different reforming processes are presented.

For all conditions examined, the equilibrium mixture comprised primarily six species—hydrogen, carbon monoxide, carbon dioxide, water vapor, methane and carbon. The other species were present

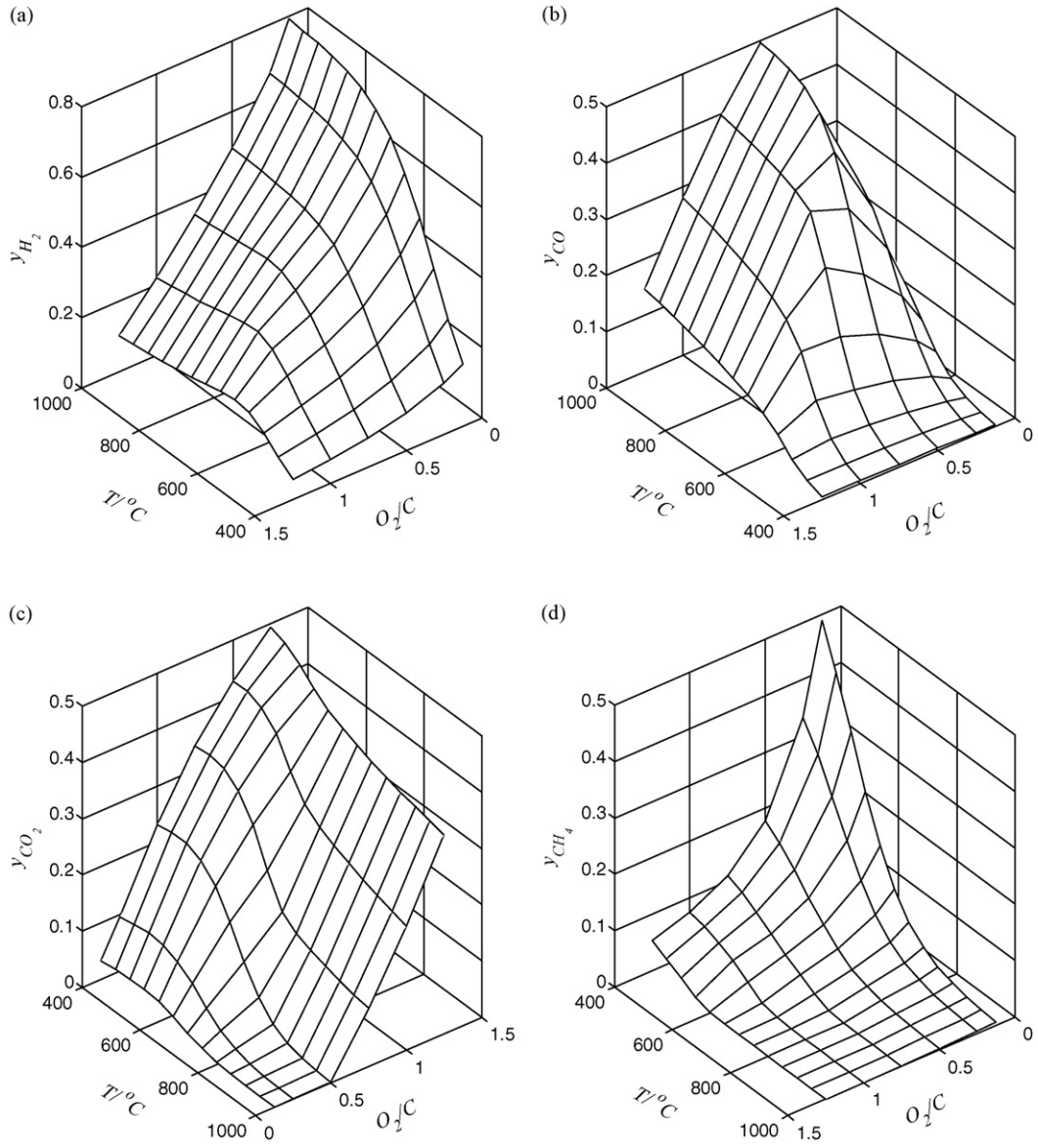

Fig. 10. Thermodynamic equilibrium gas phase product mole fraction of H_2, CO, CO_2 and CH_4 for partial oxidation at 1 atm.

at mole levels less than 1×10^{-5} moles corresponding to less than 0.001 ppm.

4.2.1. Steam reforming

The gas-phase equilibrium mole fraction for key four species – hydrogen, carbon monoxide, carbon dioxide and methane – is presented in Fig. 8 as a function of temperature and S/C ratio. It is useful to recall that the temperature range of interest for steam reforming is 600–800 °C and that the carbon-free operation requires S/C ratio of 1.75 or greater for this temperature range. However, to avoid carbon-free operation over the entire temperature range spanning the cooler temperatures in the upstream and downstream process units and tubings, a S/C ratio equal to or greater than 2 would be preferable. The influence of S/C ratio on (gas-phase) hydrogen mole fraction can be seen in Fig. 8a. Over 600–800 °C, the hydrogen mole fraction decreases with an increase in S/C ratio. In the same temperature range, the carbon monoxide and methane mole fraction also decreases whereas carbon dioxide mole fraction increases with an increase in S/C ratio. However, the methane mole fraction is less than 0.1 for S/C ratio of 1.75 or greater. Thus, the decrease in hydrogen mole fraction appears to be at the cost of increase in carbon dioxide and water mole fractions. Also, very low concentrations of H_2S, approximately 1×10^{-10} ppm is observed. The equilibrium SO_2 level is even lower ($<1 \times 10^{-20}$ ppm).

In systems where the total mole numbers change, assessing the reaction performance in terms of mole fraction can be misleading. Instead, the yield of the desirable product is a metric that should be considered. In Fig. 9, the hydrogen yield as a function of temperature for different S/C ratio is presented. Indeed, the hydrogen yields exhibit very interesting trends both with respect to S/C ratio and temperature effects. Unlike the hydrogen mole fraction trend, the hydrogen yield increases with an increase in S/C ratio. This would imply that both from carbon-free operation point-of-view and to enhance the hydrogen yields, it would be preferable to operate at S/C ratios significantly higher than 2. However, higher S/C ratio would also mean higher energy requirements for steam generation. It is also noted that over the S/C ratios of interest, the hydrogen yields levels off at higher temperature. Since, the energy requirements for high temperature operations would also be high, as will be discussed in Section 4.3, it would be preferable to operate in the 700–800 °C range.

4.2.2. Partial oxidation

In Section 4.1, it was identified that the carbon-free operation for partial oxidation is possible for the entire temperature range of interest 600–1000 °C, if O_2/C ratio is 1.1 or greater. If the POX reactor is operated at higher temperatures (900–1000 °C), a lower O_2/C ratio of 0.75 would allow carbon-free operation. The choice of O_2/C ratio should consider the hydrogen yield. The gas-phase equilibrium mole fraction for key species for POX system is presented in Fig. 10 as a function of temperature and O_2/C ratio. The hydrogen mole fraction as a function of temperature for O_2/C ratio of up to 1.25 is shown in Fig. 10a. Over 600–1000 °C, a dramatic decrease in gas-phase hydrogen mole fraction is seen with an increase in O_2/C ratio. For a given O_2/C ratio, as expected, the hydrogen mole fraction increases with an increase in temperature. Correspondingly, it can be seen from Fig. 10b that the carbon dioxide mole fraction increases and then decreases with O_2/C ratio for a given temperature and increases with an increase in temperature. The mole fraction of carbon monoxide shows a maximum around O_2/C ratio of 0.5 consistent with stoichiometry of reaction (2). Only a small amount of methane is observed at O_2/C ratio greater than 0.5 over the temperature range of operational interest (600–1000 °C). Similar to SR equilibrium compositions, very low concentrations of H_2S ($<1 \times 10^{-10}$ ppm) and SO_2 ($<1 \times 10^{-20}$ ppm) was noted.

Since hydrogen yield is an important metric for assessing reforming process, again, the hydrogen yield as a function of temperature for various O_2/C ratio is presented in Fig. 11. Several interesting observations can be made from Fig. 11. At low O_2/C ratios (<0.5), the hydrogen yields are interestingly independent of the O_2/C ratio but increase with increasing temperature. Intuitively, it was expected that for the low O_2/C ratio (<0.5), an increase in O_2/C ratio will result in a decrease in hydrogen yield since oxygen would increasingly associate with hydrogen resulting in an increase in water and a decrease in hydrogen yield. However, for these low O_2/C ratios, an increase in O_2/C ratio results in an increase in CO formation instead of H_2O formation. In fact, for O_2/C ratio $\leq$0.5, CO constitutes over 90% of oxygen-containing species.

For higher O_2/C ratios, the hydrogen yield increases rapidly with the temperature up to a certain temperature and then is nearly invariant for a further small temperature increase but thereafter decreases with an increase in temperature. The temperature at which hydrogen yields exhibits lower change in yields with temperature seems to correspond to the carbon formation boundary temperature. Further, it can be noted that at higher temperatures, for O_2/C ratios greater than 0.5, the hydrogen yields decrease with an increasing O_2/C ratio. These results show that although low O_2/C ratio would appear to be favorable for high hydrogen yields, such operating compositions offer the risk of carbon formation.

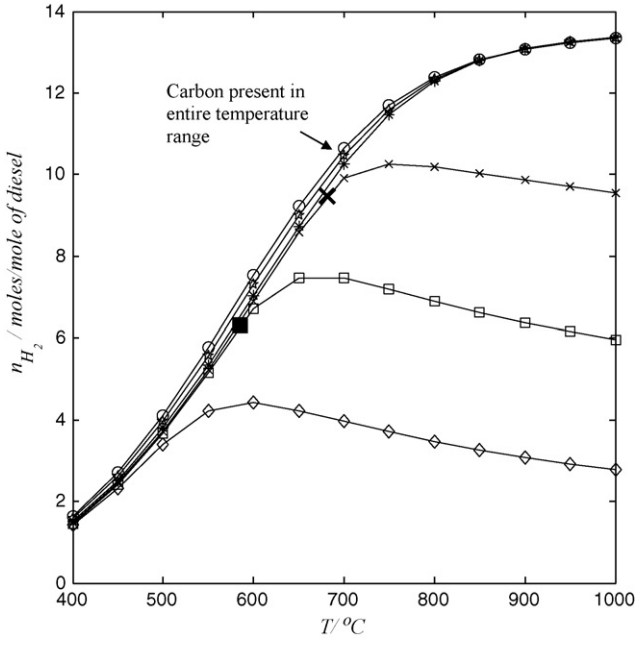

Fig. 11. Hydrogen yield for partial oxidation at 1 atm: ○, O_2/C = 0.125; +, O_2/C = 0.25; *, O_2/C = 0.5; ×, O_2/C = 0.75; □, O_2/C = 1.00; ◊, O_2/C = 1.25. (*Note*: Dark marker for O_2/C = 0.75 and O_2/C = 1.0 indicates the carbon formation boundary).

The challenge of finding the optimum O_2/C ratio for POX operations is apparent on examining the influence of O_2/C ratio in potentially carbon-free operation region. To ensure carbon-free operation in a POX reactor system, temperature in the upstream and downstream units should also be considered. In particular, the cooler entrance region of POX reactor where temperatures of 600–700 °C may exist, an O_2/C ratio of 1.2–1.25 would be required. The hydrogen yield at these high O_2/C ratios is less than half of that for other O_2/C ratios, for example, of 0.75 at a temperature of 800 °C. On the other hand, despite the high yield at 800 °C for O_2/C ratio of 0.75 thermodynamically carbon-formation can still occur. Even higher temperature operations would overcome this problem but realization of the temperature would again depend on the heat generated during the reaction which is lower for lower O_2/C ratio. Thus, a balance between carbon-free operation and maximization of hydrogen yield is required. It is recognized that these analyses do not consider kinetic effect such that carbon-free operation at lower O_2/C ratio may be possible due to kinetic suppression of carbon formation although thermodynamically this is not the case.

The results discussed above were for oxygen introduced as pure oxygen, which is commercially possible by use of pressure swing adsorption. For simplicity of operation, air instead of oxygen may be employed for generating reformate stream for fuel cell. However, there are two drawbacks of using air as oxygen source. First, in case of improper reactor operation if the oxygen goes through the reactor unreacted and ends up in the fuel cell anode, it will get oxidized at the anode creating hot spots and can damage the anode or even a cell. Second, the dilution due to the presence of nitrogen also translates into significant lowering of hydrogen partial pressure or concentration which adversely affects the reversible potential and anode electrochemical kinetics. Simulations were carried out to compute equilibrium compositions by using air instead of oxygen as a source of O_2. Similar trends with respect to temperature and O_2/C ratios were observed (results not presented) with the only observation that the hydrogen mole fraction, expectedly, were reduced.

4.2.3. Autothermal reforming

Autothermal reforming can be thought to be a combination of steam reforming and partial oxidation processes. Thus, both O_2/C and S/C ratios are available as operational parameter for control of the process output. This, however, also expands the region for exploring desirable operating conditions. To minimize redundancy, only the hydrogen yield results are discussed. Fig. 12(a–c) presents the hydrogen yields a function of S/C ratio and temperature for O_2/C ratio of 0.125, 0.25 and 0.5, respectively. From Table 2, the carbon-free operations for O_2/C ratios of 0.125, 0.25 and 0.5 is noted to be for values of S/C ratios exceeding 1.5, ~1.3 and ~0.85, respectively. Thus, examining the hydrogen yields over the temperature range of interest (600–1000 °C) in the carbon-free region, it is noted that the yields do not increase significantly with an increase in the S/C ratios. Thus, it would appear that the S/C ratio should be kept at levels as low as possible to practically avoid carbon formation. For the ease of observing the influence of O_2/C ratio, the hydrogen yield at S/C ratio of 1.75 as a function of temperature for the three different O_2/C ratios is presented (Fig. 12d). Similar to the POX results, increasing O_2/C ratio results in a significant decrease

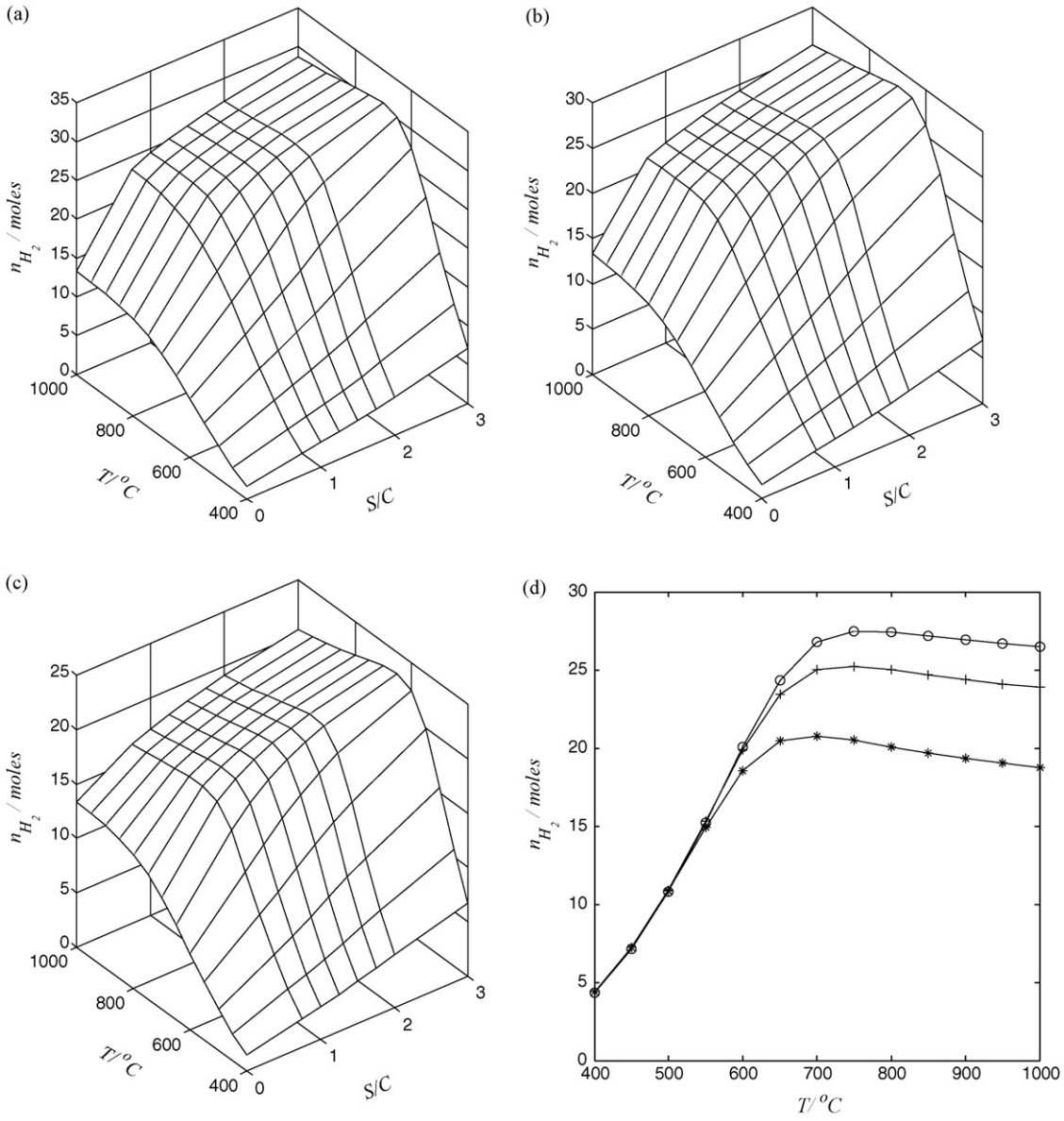

Fig. 12. Hydrogen yield (moles of hydrogen per mole of diesel) for ATR at 1 atm for S/C = 0–3 and (a) O_2/C = 0.125, (b) O_2/C = 0.25, (c) O_2/C = 0.5 and (d) hydrogen yield at S/C = 1.75; and ○, O_2/C = 0.125; +, O_2/C = 0.25; *, O_2/C = 0.5.

in the hydrogen yields. In summary, the equilibrium analyses would indicate that it is preferable to operate reactor as low as 750 °C and keep the O_2/C low (0.125–0.25) with S/C greater than 1.25 and ideally 1.75 in order to have no carbon in the entire temperature region.

4.3. Energy requirement and thermoneutral operation

In the preceding section, the ATR performance was examined purely from chemical equilibrium point. However, it is also important to consider that the ATR operations, by definition, are thermoneutral. That is, there is no external energy requirement for operating the ATR at the desirable state. To assess the energy requirements and viability of thermoneutral operation for recommended operational regime (O_2/C and S/C ratio), enthalpy calculations were carried out. The feed enthalpy was calculated assuming liquid diesel and liquid water and/or air to be fed at 25 °C as shown the system boundary in Fig. 1. The enthalpy of the equilibrated mixture at a given temperature was computed from the enthalpy data and known composition. Enthalpy data are taken from UniSim package. Diesel property was computed as that of mixture of pure hydrocarbons $C_{14}H_{30}$, $C_{15}H_{32}$, and $C_{10}H_8$ in the molar ratio 0.65:0.20:0.15, respectively.

The results of the computations for ATR and steam reforming processes are presented in Fig. 13. The energy is expressed as kJ mol^{-1} of diesel in the feed. The energy requirement of steam reforming process at various S/C ratios is presented in Fig. 13a for information sake and that for ATR at O_2/C ratios of 0.125, 0.25 and 0.5 are presented in Fig. 13b–d respectively. The zero enthalpy line indicates thermoneutral point. As expected, there is no feasible thermoneutral point for the endothermic steam reforming process. The energy requirements for SR process are significant with a considerable energy required (>30%) for vaporization of water. For example, for S/C = 1.75, T = 800 °C, heating of water from 25 to 800 °C requires 1739 kJ, which represents 41% of total endothermic heat of 4200 kJ mol^{-1} of diesel for the process.

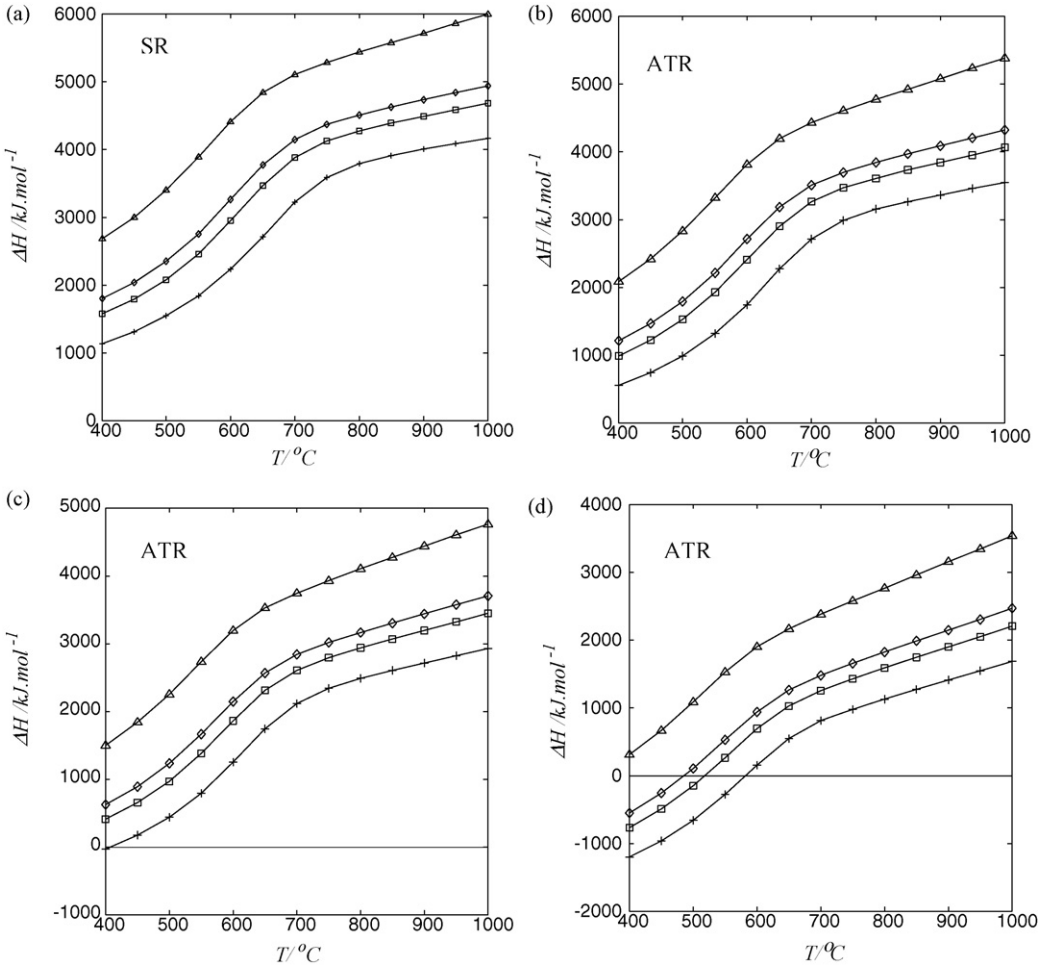

Fig. 13. Enthalpy change for SR and ATR reactor at 1 atm pressure. Feed is at 25 °C and product is at reactor temperature. (a) O_2/C = 0; (b) O_2/C = 0.125; (c) O_2/C = 0.25; (d) O_2/C = 0.50; *, S/C = 1.25; □, S/C = 1.75; ◊, S/C = 2.00; △, S/C = 3.00 (*Note*: Feed contains air).

For the ATR operation, expectedly, the energy inputs are lower than that for SR. The energy requirement reduces with an increase in O_2/C ratio. This is expected since increase in oxygen promotes presence of products of oxidation, an exothermic process. Nonetheless, it can be noted that for O_2/C ratio of 0.125, the operation is endothermic for entire temperature range and S/C ratio greater than 0.75. Upon increasing the O_2/C ratio to 0.25, thermoneutral operation at unfeasibly low temperature of 400 °C is indicated and that too at S/C ratio of 1.0 which is not high enough to avoid carbon-free operation (Fig. 13c). At a further higher O_2/C ratio of 0.5 (Fig. 13d), thermoneutral operation is possible for S/C ratios of 1.0–2.0. However, the thermoneutral operation temperature is still low in the range of 500–600 °C, which may not be feasible because of kinetic limitations of the reactions unless appropriate catalysts are found. It can be concluded that the determination of desirable operating conditions wherein carbon-free operation is ensured and hydrogen yield is maximized while energy input is minimized remains a challenging task and requires multi-variable optimization. However, we recommend that it is preferable to operate ATR at O_2/C ratio of 0.25 or little higher by supplying heat to the reformer such that hydrogen yields are maximized.

It is important to recognize that analysis in this work is on one process unit—the diesel reformer. In a larger system, energy flows for all units would have to be considered for overall process optimization. Further, many different system configurations or system integration strategies are possible requiring rigorous process system analysis. Furthermore, for a reformer coupled with a downstream fuel cell unit, different amounts of direct (e.g. radiative heat from SOFC stack to the reformer) and indirect heat (e.g. exhaust gas) will be available depending upon the type of fuel cell, its operating temperature, and its operating point (current density and cell potential),. The determination of operating conditions that maximizes either the system output or the system efficiency becomes a non-trivial task with a configuration/operating condition specific solution.

4.4. Reactions representing the overall chemical equilibrium

A few possible overall reactions for reforming are described in Section 2.2. It should be noted that the actual reaction mechanism and each reaction described in section 2.2 comprises hundreds of elementary reactions—both surface and gas-phase reactions [7]. From thermodynamics point of view, if one is interested in equilibrium composition of stable species, either a complete knowledge of reaction pathway or an intensive Gibbs minimization calculation is required. However, from the Gibbs free energy minimization calculations presented in this study, it is observed that the major species produced during reforming of diesel are hydrogen, CO, CO_2, CH_4, water and carbon. Thus, it appears that the equilibrium behavior of all three diesel reforming processes can be approximated by computing the composition of 6 species made of 3 elements—C, H and O. In other words, the equilibrium behavior of

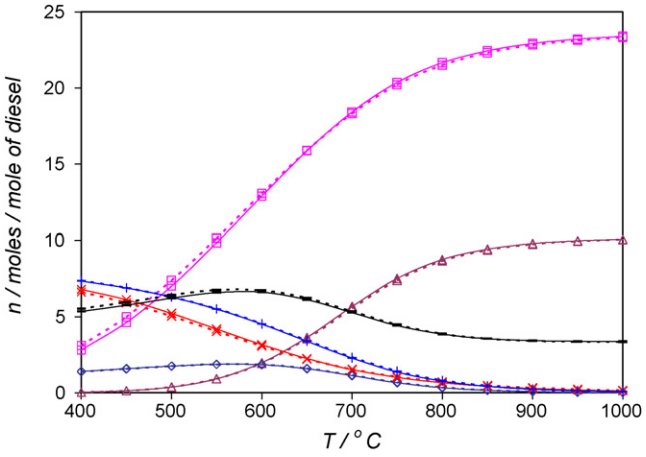

Fig. 14. Comparison of equilibrium composition predicted by Gibbs minimization and by three independent equations for major products of the reforming. S/C = 0.75, —, calculated by Gibb's minimization; - - -, calculated by solving 3 independent reactions; □, H_2; △, CO; ◊, CO_2; ×, CH_4, +, H_2O; –, C.

reforming process can be approximately defined if three independent reactions relating the 6 species are specified with 3 constraint equations imposed by the element balance. In carbon formation region, 6 major reforming species made of 3 elements can be used to describe the equilibrium behavior. That is, the degree of freedom is $6-3=3$ requiring only 3 independent reactions relating the 6 species.

Instead of choosing the reactions either *ad hoc* or by applying statistical methods, we decided to consider Eqs. (5), (6) and (11) based on the knowledge of reforming processes. However, it should be noted that any two equations out of Eqs. (4)–(7) can represent the equilibrium composition. Equilibrium computations were carried out in UniSim by considering equilibrium reactor operation and specifying the occurrence of the reactions 5, 6 and 11. The S/C ratio of 0.75 was selected to ensure the computations were inside the carbon-formation region. The equilibrium composition computed from Gibbs free energy minimization (which considers all 19 species selected in Section 3.3) is presented along with the results from the 3 reactions equilibrium reactor operation in Fig. 14. It can be noted that the composition of the six species predicted from the two different methods compares very well with each other.

Thus, the equilibrium composition for diesel reforming processes can be readily determined by applying the stoichiometric method considering the three reactions (5), (6) and (11) for which the equilibrium constant is given as follows:

$$\ln(K_{\mathrm{Eq.(5)}}) = \frac{26194}{T} - 29.4 \tag{40}$$

$$\ln(K_{\mathrm{Eq.(6)}}) = \frac{21791}{T} - 25.4 \tag{41}$$

$$\ln(K_{\mathrm{Eq.(11)}}) = -\frac{10171}{T} + 12.5 \tag{42}$$

It should be noted that the equilibrium constant are unit-less and can be related to the equilibrium activities (defined by Eq. (33)) of reactants and products.

5. Conclusions

A thermo-chemical study of reforming of commercial diesel with 50 ppm sulfur content was completed. Equilibrium composition for SR, POX and ATR was obtained by Gibbs free energy minimization routine, implemented in Matlab. A total of 19 chemical species were considered which included in addition to the expected C–H–O species—naphthacene, anthracene, graphite carbon, elemental sulfur, sulfur dioxide, sulfur trioxide, hydrogen sulfide, and sulfuric acid vapor. Equilibrium calculations for a wide range of temperature 400–1000 °C, steam to carbon ratio (S/C) of 0–3, and oxygen to carbon ratio (O_2/C) of 0–1 spanning the entire range of operations for the three modes of reforming was completed. Carbon formation boundaries were mapped and allowed the identification of carbon-free operating regimes. H_2S is found to be more favorable than SO_2 for all reforming operations and its equilibrium mole fractions is in the order of 1×10^{-10} ppm.

In case of steam reforming, high hydrogen yield with increase in temperature and S/C ratio is observed. In order to avoid the carbon formation for entire range of temperatures S/C ratio should be ≥2. It is also found that increasing the S/C ratio increases the hydrogen yield. However, the selection of S/C ratio requires a balance between maximizing hydrogen yield and minimizing energy input both of which increase with S/C.

Thermodynamic analysis suggest that partial oxidation of diesel is least favorable option as it forms high amount of carbon and in order to remain outside the carbon formation boundary, very high temperature and high O_2/C ratio is required. High O_2/C ratio further decreases the hydrogen yield. Dilution by nitrogen, if air is used, makes the process worst and mole fraction of hydrogen in the product stream is lower than 0.2.

In case of autothermal reforming, for all O_2/C ratios greater than 0.125, S/C ratio of 1.75 is ideal in order to remain in carbon free boundary for entire range of operation. For any O_2/C ratio, S/C above 1.25 marginally increases the hydrogen yield. Above 750 °C, there is very little increase in hydrogen with temperature at the cost of more CO at high temperature. The best operating condition is O_2/C in the range of 0.125–0.25 and S/C greater than 1.25, ideally 1.75 in order to have no carbon in the entire temperature region. Enthalpy analysis indicates that thermoneutral operation of ATR in carbon-free region at temperatures sufficiently high (>700 °C) for reasonable kinetics is not possible. Thus, recommended ATR operating conditions are 750 °C with O_2/C ratio 0.25 or little higher, S/C greater than 1.25 (ideally 1.75) and with constant heat supply.

Analysis of equilibrium composition for all three reforming modes indicated that only six major species – H_2, CO_2, CO, H_2O, CH_4, and C – exist. Thus, a set of three independent reactions is proposed that along with element balance equations can adequately describe the equilibrium composition for the entire range of reforming operation.

References

[1] No Breathing Room—National Illness Costs of Air Pollution, Summary Report, August 2008, Canadian Medical Association.
[2] K. Ahmed, K. Foger, Electrochem. Soc. Proc. 7 (2003) 1240–1249.
[3] D. Liu, T.D. Kaun, H.K. Liao, S. Ahmed, Int. J. Hydrogen Energy 29 (2004) 1035–1046.
[4] M.V. Mumdschau, C.G. Burk, D.A. Gribble, Catal. Today 136 (2008) 190–205.
[5] Argonne National laboratory, 2007, http://www.transportation.anl.gov/engines/idling.html (accessed October 25, 2008).
[6] C.H. Bartholomew, Catal. Rev. Sci. Eng. 24 (1982) 67–112.
[7] D. Shekhawat, D.A. Berry, T.H. Gardner, J.J. Spivey, Catalysis 19 (2006) 184–253.
[8] A.E. Lutz, R.W. Bradshaw, J.O. Keller, D.E. Witmer, Int. J. Hydrogen Energy 28 (2003) 159–167.
[9] A.E. Lutz, R.W. Bradshaw, L. Broomberg, A. Rabinovich, Int. J. Hydrogen Energy 29 (2004) 809–816.
[10] A. Lindetrmeir, S. Kah, S. Kavurucu, M. Muhlner, Appl. Catal. B: Environ. 70 (2007) 488–497.
[11] I. Kang, J. Bae, J. Power Sources 159 (2006) 1283–1290.
[12] I. Kang, J. Bae, G. Bae, J. Power Sources 163 (2006) 538–546.
[13] G.A. Olah, A. Molnar, Hydrocarbon Chemistry, Wiley, New York, 1995.
[14] G. Kolb, Fuel Processing for Fuel Cells, Wiley, Weinheim, 2008.
[15] Z. Sahin, Energy Fuels 22 (2008) 3201–3212.
[16] L.F. Brown, Int. J. Hydrogen Energy 26 (2001) 381–397.

[17] J.C. Amphlett, R.F. Mann, B.A. Peppley, P.R. Roberge, A. Rodrigue, J.P. Salvador, J. Power Sources 71 (1998) 179–184.
[18] J.H. Wang, M. Liu, Electrochem. Commun. 9 (2007) 2212–2217.
[19] P.K. Cheekatamarla, A.M. Lane, J. Power Sources 154 (2006) 223–231.
[20] W.R. Smith, R.W. Missen, Chemical Reaction Equilibrium Analysis: Theory and Algorithms, Cambridge University Press, London, 1982.
[21] E.Y. Garcia, M.A. Laborde, Int. J. Hydrogen Energy 16 (1991) 307–312.
[22] M.W. Chase, NIST-JANAF Thermochemical Tables, J. Phys. Chem. Ref. Data (1998) (Monograph 9).
[23] K.M. Pamidimukkala, D. Rogers, G.B. Skinner, J. Phys. Chem. Ref. Data 11 (1982) 83–99.
[24] C.L. Yaws, Chemical Properties Handbook, McGraw-Hill, New York, 1999.
[25] M. Cimenti, J.M. Hill, J. Power Sources 186 (2009) 377–384.